Route towards finding large magnetic anisotropy in nanocomposites: Application to a $W_{1-x}Re_x$/Fe multilayer

Sumanta Bhandary,[1] Oscar Grånäs,[1] Laszlo Szunyogh,[2] Biplab Sanyal,[1] Lars Nordström,[1] and Olle Eriksson[1]
[1]*Department of Physics and Astronomy, Uppsala University, Box 516, SE-751 20 Uppsala, Sweden*
[2]*Department of Theoretical Physics, Budapest University of Technology and Economics, Budafoki u. 8, H-1111 Budapest, Hungary*
(Received 9 August 2011; published 9 September 2011)

We suggest here a nanolaminate, 5[Fe]/2[W_xRe_{1-x}] ($x = 0.6$–0.8), with enhanced magnetic hardness in combination with a large saturation moment. The calculated magnetic anisotropy of this material reaches values of 5.3–7.0 MJ/m^3, depending on alloying conditions. We also propose a recipe in how to identify other novel magnetic materials, such as nanolaminates and multilayers, with large magnetic anisotropy in combination with a high saturation moment.

DOI: 10.1103/PhysRevB.84.092401 PACS number(s): 75.10.Lp, 75.30.Cr, 75.30.Gw, 75.40.Mg

I. INTRODUCTION

The search for new materials with tailored properties for specific applications is a vital effort in the realization of novel and improved technologies. Recent developments in the ability to perform theoretical simulations with predictive power are just starting to show potential in this regard. An example here is the predicted huge tunneling magnetoresistance (TMR) of Fe/MgO/Fe trilayers,[1,2] which subsequently was verified experimentally.[3] Most read heads in modern disk drives actually make use of this huge TMR effect.

Magnetic materials are found in many applications. An example is permanent magnets, where the large energy product of $Nd_2Fe_{14}B$ is utilized,[4] e.g., in electrical machines and generators. The material properties which are relevant in $Nd_2Fe_{14}B$ are the large magnetic anisotropy energy (MAE) combined with a large saturation moment (M_s). Recently the risk of only a limited access to rare-earth elements has been discussed, with a potential threat for manufacturing permanent magnets such as $Nd_2Fe_{14}B$.[5] Other classes of materials, which do not contain rare-earth elements, but with similar magnetic properties, are hence in high demand.

To identify materials with a large saturation moment only, is a subject of interest in its own right, with several challenges, e.g., as discussed recently.[6] The wish of combining a large saturation moment with a high MAE becomes even more complicated, since the physical interactions responsible for one property do not necessarily correlate with those determining the other. To date no material has been identified with magnetic properties superior to rare-earth-based compounds, where $SmCo_5$ and $Nd_2Fe_{14}B$ stand out, in particular. Several new materials have, however, been considered, where the tetragonal compound FePt is one of the most recently studied materials.[7]

Theory based on density functional theory has proven accurate in reproducing measured saturation moments, and the difference between observations and measurements is seldom larger than 5–10 %. As regards the magnetic anisotropy, it is significantly more difficult, since the accuracy needed is very high. However, some developments have recently been made.[8] As an example we mention the predicted large MAE of a tetragonally strained FeCo alloy[9] which subsequently was verified experimentally.[10]

In this Brief Report we use first-principles theory and focus on the MAE and suggest a nanolaminate with enhanced magnetic hardness in combination with a large saturation moment. In addition to identifying this material, we propose here a recipe in how to identify other novel magnetic materials, such as nanolaminates and multilayers, with large magnetic anisotropy in combination with a high saturation moment.

II. GEOMETRY AND COMPUTATIONAL DETAILS

In a similar spirit as that used in Ref. 9, we wish to investigate the MAE as a function of electron concentration, but in the present study it is the electron concentration of the ligand atoms, W and Re, which are under focus, not the atoms carrying the magnetic moment (Fe). The advantage of tuning the electron concentration of the ligand states is that they can be chosen with a large spin-orbit coupling, which via hybridization with the Fe 3*d* states are expected[11] to influence the anisotropy of the whole multilayer. We considered multilayers of different thicknesses of the Fe and W-Re layer, and the chosen composition 5[Fe]/2[W_xRe_{1-x}] ($x = 0.6$–0.8) is the one that gives a suitable strain of the W-Re layer, as well as an optimized electron concentration, as described below. The final geometry was obtained via force minimization using the VASP package. This resulted in essentially a tetragonal structure with an effective c/a ratio of the W-Re layers (and of the Fe layers), i.e., the ratio between atomic distances of the W-Re layer in the out-of-plane and in-plane directions. As we shall see below, this ratio is a crucial parameter determining the MAE.

Using the geometry optimized structure we then used two all-electron methods to calculate the MAE, which are described in detail below. The two methods are below referred to as FPLMTO-VCA[12] and KKR-CPA.[13] In these calculations we also varied, within limits, the c/a ratio of the W-Re layer, and as we shall see below, this causes drastic changes in the MAE. An experimental realization of modifying the effective c/a ratio of multilayers is, in general, readily done by varying the thickness of the individual layers.

As mentioned, from the geometry optimized structure we used an all-electron, full-potential linear muffin-tin orbital (FPLMTO) method[12] to evaluate the MAE. This calculation used the simple virtual crystal approximation (VCA) to

treat the alloying between W and Re. In these subsequent calculations we also varied, within limits, the c/a ratio of the W-Re layer, and as we shall see below, this causes drastic changes in the MAE. An experimental realization of modifying the effective c/a ratio of the W-Re layers can be done by tuning the relative amount of Fe and W-Re layers, i.e., by considering the superlattice m[Fe]/n[W_xRe_{1-x}], with $m \neq 5$ and $n \neq 2$.

In order to give further credit to our theoretical study we repeated the MAE calculations for the 5[Fe]/2[W_xRe_{1-x}] superlattice in terms of the fully relativistic screened Korringa-Kohn-Rostoker (SKKR) method.[13] This method can combine a full relativistic description with the more advanced coherent-potential approximation (CPA) to tackle the chemical disorder in the W_xRe_{1-x} layers (where x = 0.79). We used the local spin-density approximation of the density functional theory as parametrized by Vosko *et al.*;[14] the effective potentials and fields were treated within the atomic sphere approximation (ASA) with an angular momentum cut-off of $\ell_{max} = 3$. To calculate the MAE we used the so-called *magnetic force theorem*[15] in which the previously determined self-consistent effective potentials and fields are kept fixed and the change of total energy of the system with respect to the direction of the magnetization, $\hat{n}$, is approached by that of the single-particle (band) energy. In these calculations the energy integrations were performed by sampling 20 points on a semicircular path in the upper complex semiplane, and for the energy point closest to the real axis, nearly 10 000 k points were selected in the surface Brillouin zone that ensured a numerical error not exceeding about 5% of the calculated MAE values.

III. RESULTS

We show in Fig. 1(a) the calculated MAE of 5[Fe]/2[W_xRe_{1-x}] as a function of the local c/a ratio of the W-Re layers. The starting concentration which was considered was $x = 0.8$. In the figure we show both results from FPLMTO-VCA as well as KKR-CPA. From the figure it is clear that the two methods give similar overall behavior, but that the KKR-CPA calculations result in a maximum of ~ 4 meV/f.u., whereas the FPLMTO-VCA results have a maximum of $\sim$3 meV/f.u. This is comforting since the KKR-CPA treats the disorder better, while the FPLMTO-VCA handles the relaxed structure more accurately. The two methods give both a similar shape of the MAE curve with respect to the c/a ratio of the W-Re layer, and the maximum of the curves occur at similar c/a. The maximum value of the KKR-CPA results can be compared to the MAE of FePt, which from theory is $\sim$3 meV/f.u.,[16] whereas experiment results in 1.2 meV/f.u.[17] The MAE of 5[Fe]/2[$W_{0.8}Re_{0.2}$] is hence very comparable to that of FePt. A further tuning of the magnetic anisotropy can be done by modifying the amount of alloying between W and Re in the multilayer, while keeping the c/a ratio the same as that giving the maximum MAE value in Fig. 1, i.e., 1.34. Calculations based on FPLMTO-VCA are shown in Fig. 1(b), and we note that the MAE can be made $\sim$30% larger by tuning x to 0.6.

As to the magnetic moments, they are rather constant for the different values of x considered, and we obtain values of $1.65\mu_B$ per interface atom and $2.4\mu_B$ for the subinterface Fe atoms, and $2.2\mu_B$ for the Fe atom in the middle of the Fe slab.

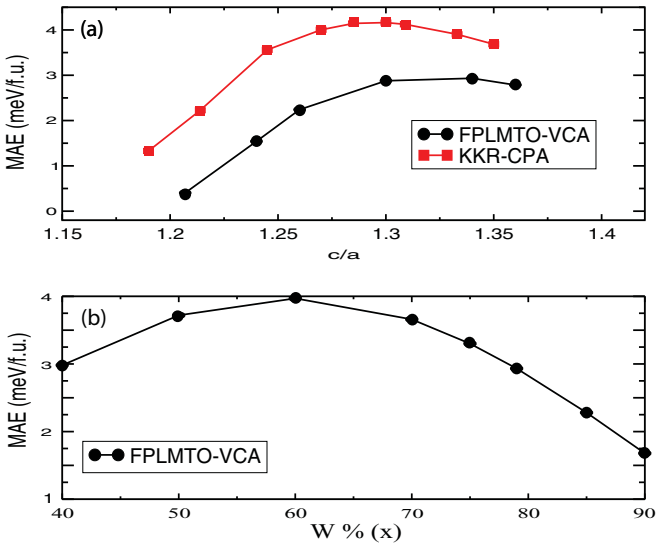

FIG. 1. (Color online) (a) Calculated magnetic anisotropy of 5[Fe]/2[W_xRe_{1-x}] ($x = 0.8$) as a function of the effective c/a ratio of the W-Re layers. (b) Calculated magnetic anisotropy of 5[Fe]/2[W_xRe_{1-x}] as a function of W concentration, x, for a c/a ratio of 1.34 of the W-Re layers. The MAE is shown per formula unit.

The moment on W-Re is $-0.1\mu_B$, resulting in a total moment just above $10\mu_B$/f.u. For comparison we note that for FePt this value is $3.3\mu_B$/f.u.

So far we have only considered calculated values per formula unit, whereas for practical applications, with respect to volume, one should compare the 5[Fe]/2[W_xRe_{1-x}] system with, e.g., FePt. As concerns the MAE, we obtain a maximum value 5.3–7.0 MJ/m^3 (depending on concentration or computational method) which should be compared to a measured value of $\sim$7 MJ/m^3 for FePt.[7] For the moments we obtain $0.11\mu_B$/Å^3 which is to be compared to $0.12\mu_B$/Å^3 for FePt. A final note on the comparison to the properties of FePt, is that this material often exhibits partial chemical disorder on the Fe and Pt sublattices, which drastically reduces the MAE.[18]

In order to obtain a more detailed, microscopical understanding for why the MAE of Fig. 1 obtains a maximum at c/a close to 1.3, we show first of all that the large MAE is caused by the large spin-orbit coupling of the W-Re atoms. As a second step we will illustrate that it is a delicate detail of the energy bands of the W-Re layer, which take a special structure for a c/a ratio close to 1.3, which determine the large MAE. We start, however, with analyzing the spin-orbit effect of the W-Re atoms.

As a direct way to illustrate the dominant role of the W_xRe_{1-x} layers in the formation of the high perpendicular MAE of this system, we varied the spin-orbit coupling (SOC) strength at these layers for the optimal c/a ratio ($c/a = 1.3$) and concentration (for $x = 0.8$, other values of x give a similar picture). Here we employed the technique developed by Ebert *et al.* within the KKR formalism.[19] The corresponding MAE values are shown in Fig. 2 for SOC strengths (ξ) scaled from 0 to 1. Remarkably, for $\xi = 0$, i.e., when SOC is considered just in the Fe layers, the MAE is slightly negative preferring thus an in-plane orientation of the magnetization. Increasing

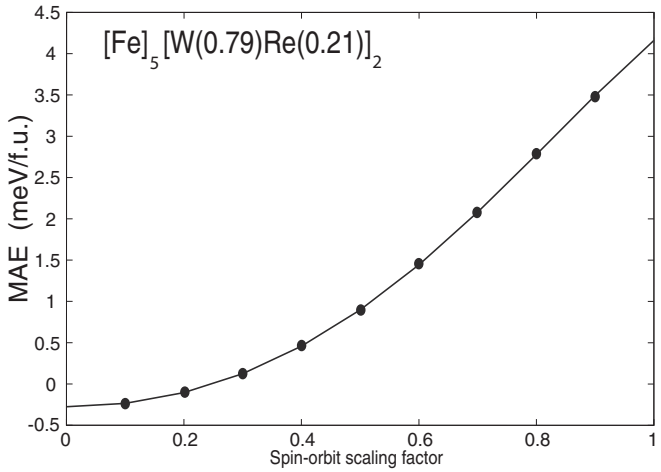

FIG. 2. Calculated MAE (circles) within the KKR-CPA approach with SOC strength scaled between 0 and 1. The optimal setup, $c/a = 1.3$ and $x = 0.8$, is fixed for the 5[Fe]2[W_xRe_{1-x}] superlattice. The solid line serves as a guide for the eyes.

ξ in the W_xRe_{1-x} layers, the MAE starts to increase as a quadratic function: this behavior is well understood in terms of the second-order perturbation theory, discussed below. For about $0.5 < \xi < 1$, however, the MAE seems to follow a linear behavior implying that in this regime SOC cannot be regarded as a small second-order perturbation to the scalar-relativistic spin-polarized band structure. Overall, the data of Fig. 2 demonstrate that the large MAE is indeed caused by the large spin-orbit coupling of the W-Re atoms.

We now turn to investigating why an effective c/a ratio of the W-Re layer close to 1.3 causes a maximum value of the MAE. The MAE of a nanocomposite material can be expressed as

$$\Delta E_{\mathrm{SO}} = \sum_{qq'} \Delta E_{qq'} = \sum_{qq'} [E_{qq'}(\hat{n}_1) - E_{qq'}(\hat{n}_2)], \qquad (1)$$

where q is the atomic species and $\hat{n}_i$ are two spin-quantization axes, one out of plane and one in plane. Each of the $E_{qq'}(\hat{n})$ can now, according to second-order perturbation theory, be written as

$$E_{qq'}(\hat{n}) = -\sum_{\mathbf{k}ij} \sum_{\{s\}} \sum_{\{m\}} n_{\mathbf{k}is,qm,q'm'} n_{\mathbf{k}js',q'm'',qm''} \times \frac{\langle qms|H_{\mathrm{SO}}(\hat{n})|qm'''s'\rangle \langle q'm''s'|H_{\mathrm{SO}}(\hat{n})|q'm's\rangle}{\epsilon_{\mathbf{k}j} - \epsilon_{\mathbf{k}i}}, \qquad (2)$$

where $\mathbf{k}$ represents the sampling points in the Brillouin zone, i,j is the occupied and unoccupied states, $\{s\} = \{s,s'\}$ run over the spin components, and $\{m\} = \{m,m',m'',m'''\}$ run over the magnetic quantum numbers. The basis functions $|qlms\rangle$ are specified through the atomic site q, the l, m, and s quantum numbers, i.e., the azimuthal, magnetic, and spin component quantum numbers. Note that the band character $n_{\mathbf{k}is,qm,q'm'}$ includes hybridization, i.e., mixing of different basis functions at, e.g., different atomic sites q. The contributions from Eq. (2) are seen to become large if the energy difference between occupied and unoccupied electron states is small enough to permit a strong coupling of the spin-orbit interaction,

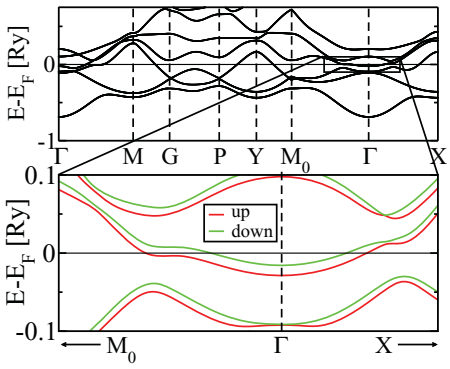

FIG. 3. (Color online) Non-spin-polarized bands (upper panel) and spin-split bands (lower panel) of W-Re for bct c/a ratio 1.3.

especially if this happens for a large fraction of the BZ. This fact is further enhanced if the states that couple via the spin-orbit coupling have a significant contribution from the states residing on the heavy W-Re atom, since this guarantees that at least one of the spin-orbit matrix elements in Eq. (2) is then large.

It is in such an analysis that the effective c/a ratio of W-Re close to 1.3 becomes clear. Inspection of a W-Re alloy reveals that as a function of the c/a ratio, conspicuous features of the band structure explain the enhanced MAE. To illustrate this, we show in Fig. 3 the energy bands along Γ-M-G-P-Y-M_0-Γ-X (of the body-centered-tetragonal BZ) of a W-Re alloy (calculated in this case byVCA, and with $x = 0.8$). From the figure one may note a spin-degenerate band situated very close to the Fermi level (E_{F}) between M_0 and Γ and X. As a function of changing the c/a ratio this band moves from being completely occupied to becoming unoccupied, and for $c/a = 1.3$ it is situated right at E_F. When put in contact with Fe, in the 5[Fe]/2[W_xRe_{1-x}] multilayer, the narrow band discussed in Fig. 3 will become exchange split, due to the induced moment of the W-Re layers. In order to illustrate this effect in a simple way, we have performed a fixed spin moment calculation of W-Re, with the same induced moment on the W-Re site as for the 5[Fe]/2[W_xRe_{1-x}] multilayer. The resulting dispersion relationship is also shown in Fig. 3 (bottom panel). Here we note a breaking of the spin degeneracy close to E_F, and the flat band is split into up and down bands, which for a substantial part of the BZ are situated on each side of E_F in a large part of the in-plane Brillouin zone. Spin-orbit coupling via the $l_+s_- + l_-s_+$ terms of H_{SO} in Eq. (2) then provides a large contribution to the magnetic anisotropy. A modification of the c/a ratio away from this value moves the flat bands away from E_F, which reduces the MAE.

IV. CONCLUSION

We have here presented theoretical evidence for a nonlaminate involving W-Re layers in contact with Fe, can result in a magnetic material with a substantial magnetic moment and a large magnetic anisotropy. The new material compares in performance to the well-known material FePt, both in terms of saturation moment as well as anisotropy. One advantage with the present system is the possibility to tune the MAE by tuning the local c/a ratio of the W-Re layer, which can be done by

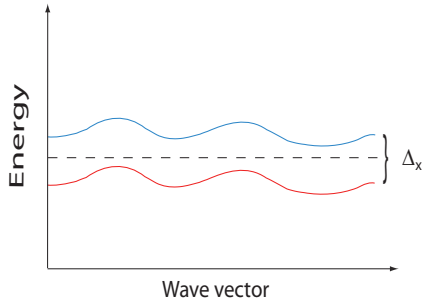

FIG. 4. (Color online) Schematic picture of the electronic structure of bands projected on heavy atoms, having the possibility of inducing a large magnetic anisotropy. Majority spin states are shown in red (lower band), minority states in blue (upper band), and the Fermi level is denoted by a dashed horizontal line. The exchange splitting is marked as Δ_x.

introducing more Fe layers. This simultaneously also increases the saturation moment per volume.

Our analysis points to a general route to find materials with a large magnetic anisotropy. A strong ferromagnetic material, preferably based on Fe or an FeCo alloy, should be in contact with a heavier material with large spin-orbit splitting. Most crucially, the electronic structure of the heavy material should be similar to the schematic energy band plot of Fig. 4. Here, bands which are dominated by states on the heavy atom are drawn to be exchange split, due to the interaction (hybridization) of the ferromagnetic material. If a large fraction of the BZ has majority bands below the Fermi level, and a large fraction of the BZ has minority states above (as drawn in Fig. 4), then the spin-orbit coupling of the heavy atom will give rise to a large contribution to the MAE for many wave vectors [as Eq. (2) shows].

The situation shown in Fig. 4 corresponds to a set of narrow bands close to the Fermi level, which corresponds to a system with a large value of the density of states at the Fermi level [DOS(E_F)]. Hence, a large value of DOS(E_F) is also a requirement when searching for novel materials with a large MAE. Unfortunately, a large value of DOS(E_F) is often associated with an unstable or metastable crystal structure,[20] which points out that it is metastable systems, such as multilayers and nanolaminates, that one should consider when searching for novel materials with a large MAE.

ACKNOWLEDGMENTS

We gratefully acknowledge financial support from the Swedish Research Council (VR), Swedish Foundation for Strategic Research (SSF), Göran Gustafssson Foundation, Carl Tryggers Foundation, STEM, and STINT. In addition, O.E. is grateful to the ERC (Project No. 247062-ASD) and KAW Foundation for support. Support from eSSENCE and STANDUP acknowledged. We also acknowledge Swedish National Infrastructure for Computing (SNIC) for the allocation of time in high performance supercomputers. Partial financial support was also provided by the Hungarian Research Foundation (Contract Nos. OTKA 84078, K68312, K77771, and IN83114) and by the New Szechenyi Plan of Hungary (Project ID: TÁMOP-4.2.1/B-09/1/KMR-2010-0002).

[1] W. H. Butler, X. G. Zhang, T. C. Schulthess, and J. M. MacLaren, Phys. Rev. B **63**, 54416 (2001).
[2] J. Mathon and A. Umerski, Phys. Rev. B **63**, 220403 (2001).
[3] S. Yuasa, T. Nagahama, A. Fukushima, Y. Suzuki, and K. Ando, Nat. Mater. **3**, 868 (2004).
[4] *Rare-Earth Iron Permanent Magnets*, edited by J. M. D. Coey (Clarendon, Oxford, 1996).
[5] D. Kramer, Phys. Today **63**(5), 22 (2010).
[6] B. Sanyal, C. Antoniak, T. Burkert, B. Krumme, A. Warland, F. Stromberg, K. Fauth, H. Wende, and O. Eriksson, Phys. Rev. Lett. **104**, 156402 (2010).
[7] S. Sun, C. B. Murray, D. Weller, L. Folks, and A. Moser, Science **287**, 1989 (2000).
[8] L. Szunyogh, B. Ujfalussy, and P. Weinberger, Phys. Rev. B **51**, 9552 (1995).
[9] T. Burkert, L. Nordström, O. Eriksson, and O. Heinonen, Phys. Rev. Lett. **93**, 27203 (2004).
[10] G. Andersson, T. Burkert, P. Warnicke, M. Björck, B. Sanyal, C. Chacon, C. Zlotea, L. Nordström, P. Nordblad, and O. Eriksson, Phys. Rev. Lett. **96**, 37205 (2006).
[11] C. Andersson, B. Sanyal, O. Eriksson, L. Nordström, O. Karis, D. Arvanitis, T. Konishi, E. Holub-Krappe, and J. H. Dunn, Phys. Rev. Lett. **99**, 177207 (2007).
[12] J. M. Wills, M. Alouani, P. Andersson, A. Delin, O. Eriksson, and A. Grechnev, in *Full-Potential Electronic Structure Method, Energy and Force Calculations with Density Functional and Dynamical Mean Field Theory*, Springer Series in Solid-State Sciences Vol. 167 (Springer, Berlin Heidelberg, 2010).
[13] J. Zabloudil, R. Hammerling, L. Szunyogh, and P. Weinberger, in *Electron Scattering in Solid Matter*, Springer Series in Solid-State Sciences Vol. 147 (Springer, Heidelberg, 2005).
[14] S. H. Vosko, L. Wilk, and M. Nusair, Can. J. Phys. **58**, 1200 (1980).
[15] H. J. F. Jansen, Phys. Rev. B **59**, 4699 (1999).
[16] G. H. O. Daalderop, P. J. Kelly, and M. F. H. Schuurmans, Phys. Rev. B **44**, 12054 (1991).
[17] S. Okamoto, N. Kikuchi, O. Kitakami, T. Miyazaki, Y. Shimada, and K. Fukamichi, Phys. Rev. B **66**, 024413 (2002).
[18] J. B. Staunton, S. Ostanin, S. S. A. Razee, B. L. Gyorffy, L. Szunyogh, B. Ginatempo, and E. Bruno, J. Phys.: Condens. Matter **16**, S5623 (2004).
[19] H. Ebert, H. Freyer, and M. Deng, Phys. Rev. B **56**, 9454 (1997).
[20] H. L. Skriver, Phys. Rev. B **31**, 1909 (1985).